

We are IntechOpen, the world's leading publisher of Open Access books Built by scientists, for scientists

6,900

Open access books available

186,000

International authors and editors

200M

Downloads

Our authors are among the

154

Countries delivered to

TOP 1%

most cited scientists

12.2%

Contributors from top 500 universities



WEB OF SCIENCE™

Selection of our books indexed in the Book Citation Index
in Web of Science™ Core Collection (BKCI)

Interested in publishing with us?
Contact book.department@intechopen.com

Numbers displayed above are based on latest data collected.
For more information visit www.intechopen.com



Design and Preparation of Nanostructured Prussian Blue Modified Electrode for Glucose Detection

Wanqin Jin, Zhenyu Chu and Yannan Zhang

*State key laboratory of Materials-Oriented Chemical Engineering,
Nanjing University of Technology
China*

1. Introduction

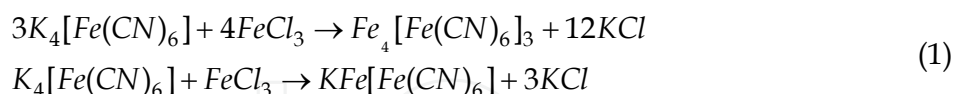
High sensitivity and anti-interference ability are critical parameters in glucose biosensor design, because of the complexity of blood composition. Prussian blue (PB) is a hexacyanoferrate with two different iron valences (+2 and +3) and was initially developed as a blue pigment in the 1700s (Bartoll, 2008). Recently researchers found that PB is an excellent material for use in the fabrication of glucose biosensors, because of its non-toxicity, high electrocatalytic activity, and low overpotential detection (Ricci & Palleschi, 2005; Karyakin et al., 2007; Wang, 2008). During glucose detection, hydrogen peroxide (H_2O_2) is produced via the enzymatic oxidation of glucose. Subsequently, PB reduces the H_2O_2 and transfers the electrons to generate a current response on the electrode surface. Thus, PB is the mediator of electron transfer in the detection process, making the electron sensitivity of PB - a key component of biosensor performance.

Chemical deposition and electrodeposition are the main processes used to synthesize a PB film on the electrode surface (Itaya et al., 1982; Zakharchuk et al., 1995). However, the sensitivity of the electrode modified with a PB film cannot be controlled, because of difficulties in film construction. Millward et al. (2001) used a self-assembly approach to deposit a PB film on a gold electrode, which greatly accelerated the development of PB-based biosensors. The advantages of applying nanostructured materials for improving biosensor performance have been recognized in recent years, especially for improving sensitivity (Cella et al., 2010; Cao et al., 2010). The utilization of nanoparticles can enhance electrode performance, even if the same materials are used. We developed a PB nanostructure to produce a high sensitivity biosensor for glucose detection, which can be directly grown on the electrode surface.

We previously synthesized PB nanoparticles on a platinum (Pt) electrode surface using a self-assembly approach (Liu et al., 2009). We found that the size and quantity of PB particles greatly affected H_2O_2 detection performance. After immobilization of the glucose enzyme, this type of biosensor was sensitive to trace concentrations of glucose in solution (Liu et al. 2009). However, it was difficult to form a regularly structured PB particle film, when synthesis was conducted via self-assembly. Thus, we further developed the self-assembly approach to deliver a novel method for obtaining a regular film of PB crystals, are thereby improving biosensor sensitivity and effectiveness.

2. Mechanism of H₂O₂ detection

PB is typically produced from a reaction between two compounds, K₄[Fe(CN)₆] and FeCl₃ (see equation 1).



KFe[Fe(CN)₆] and Fe₄[Fe(CN)₆]₃ are soluble and insoluble PB, respectively, and both species are required. The unit cell of PB is a face-centered cubic structure with lattice parameters, a = b = c = 10.143 Å. It is interesting that neighboring iron ions have different valences. The Fe²⁺ ion, in the Fe(CN)₆⁴⁺ complex, is readily reduced to the Fe³⁺ ion. The signal generated by electron transfer from Fe(CN)₆⁴⁺ is generally used in electrochemical detection to characterize the properties of the PB film.

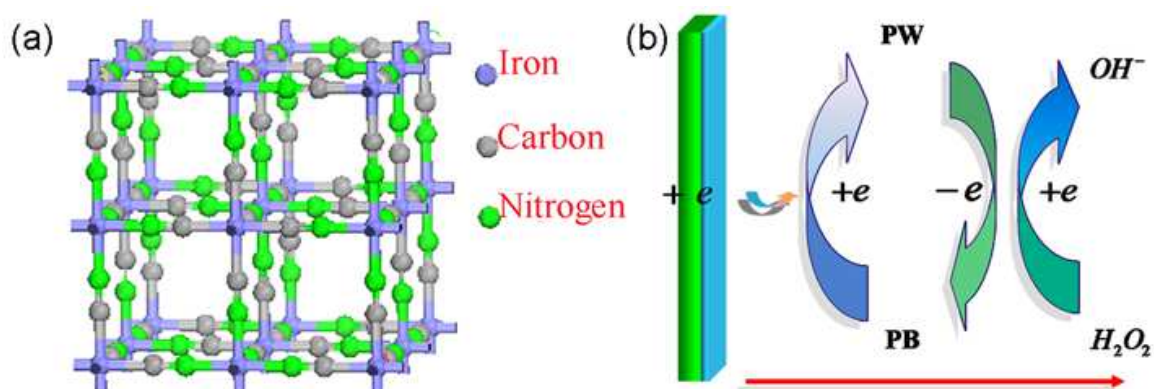


Fig. 1. (a) The structure of the PB unit cell. (b) Mechanism of H₂O₂ detection.

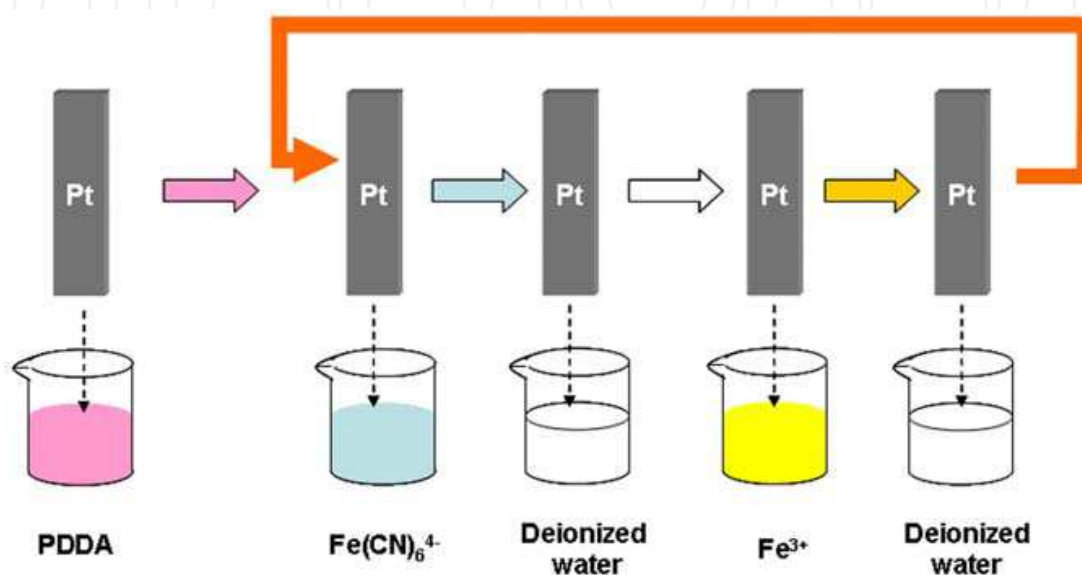
PB has two functions when used as a material in biosensor fabrication, i.e., electrocatalysis and electron transfer: When a potential (typically -0.05 V) is imposed on a PB modified electrode, the PB will acquire electrons and move into its reduced state, Prussian White (PW). If H₂O₂ is present in the detection system, PW rapidly reduces H₂O₂ to OH⁻. After donating electrons, PW reverts back to PB (Fig. 1). The direction of electron transfer during this process is from the electrode surface to H₂O₂. Thus, electrocatalysis and electron transfer determine overall electrode performance.

Regular crystalline structure is a morphological feature that has been widely demonstrated to enhance catalytic ability (Liu et al., 2010; Prevot et al., 2011). However, it is difficult to control regular PB crystal growth using conventional preparative methods, because of its rapid reaction rate during crystal formation. Consequently, novel methods are required to facilitate the regular crystal structure growth in the PB film.

3. PB crystal formation using a self-assembly approach

Self-assembly is a common approach for production of PB-modified electrodes. Scheme 1 shows the process of PB synthesis, which starts with a pre-coating layer of polyelectrolyte, to provide electrostatic adsorption sites, followed by dipping the electrode into a reactive solution for PB formation. Poly(diallyldimethylammonium chloride) (PDDA) is typically

applied as the cation polyelectrolyte layer (Hornok & Dékány, 2007; Li et al., 2008). This layer provides a foundation for further layer deposition, which means that its properties are essential for regular PB growth. The regular structure of PB is not readily formed *via* self-assembly, but this approach has been successfully applied to regular crystal growth for other materials (Wang et al., 2009; Guang et al., 2009). The PB self-assembly problem might be attributable to first layer selection, and temperature can greatly affect polymer properties. We determined the optimum method for regular crystal formation in a PB film by controlling PDDA load temperature.



Scheme 1. Production of a PB-modified electrode using a self-assembly method.

We investigated the properties of PDDA layer with respect to changes in temperature, prior to the self-assembly of PB. Electrochemical impedance spectroscopy (EIS facilitates observation of the structure and charge transfer behavior of polymer films. We compared the impedances of bare Pt and the electrodes loaded by PDDA at different temperatures. Electron transfer is essential for sensitivity in the detection of H_2O_2 . However, PDDA is not an excellent mediator for electron transfer, but we were more concerned with the resistance provided by the PDDA layer. Fig. 2 shows the results of impedance experiments, illustrating the electrode property at high frequencies due to the electron transfer kinetics of redox species at the electrode surface. The linear region is dominated by the mass transfer of probe species from the bulk solution to the interface region. We found that increasing the adsorption temperature led to a reduction in interface resistance. We compared the exact resistance values using a classical Randles circuit (inset of Fig. 2), the results of which were applied to fitting the EIS curves. The values of R_{ct} which resulted in electron transfer ability were calculated as 4.741, 5.932, 9.722, 11.47, and 13.03 Ω respectively, for the bare Pt electrode, and the electrode with PDDA adsorbed at 35, 30, 25, and 20 $^\circ\text{C}$. The resistance of the unmodified Pt electrode was the lowest, and the addition of PDDA gradually decreased the electron transfer ability. The impedance was enhanced by a reduction of the PDDA adsorption temperature. The fluidity of the polymer was very poor at low temperatures, which led to severe surface aggregation of the substrate with detrimental effects on PB assembly. This prompted the investigation of surface coverage. The fractional electrode coverage rate (θ) of PDDA was estimated according to equation 2.

$$\theta = 1 - \frac{R_{ct}^{bare}}{R_{ct}^{PDDA}} \quad (2)$$

Where R_{ct}^{bare} is the charge transfer resistance value for the bare Pt electrode, and R_{ct}^{PDDA} is the same value for the PDDA modified electrode at different adsorption temperatures. The calculated results were 0.2062, 0.5123, 0.5867, and 0.6361 for 35, 30, 25, and 20 °C, respectively. By combining these results with the resistance results, we determined why resistance did not decrease as a function of temperature increase. PDDA did not cover the whole Pt surface and electrons preferred to transfer in areas without polymer because of the lower resistance. Local preferences for electron transfer resistance were consistent with variations in polymer coverage.

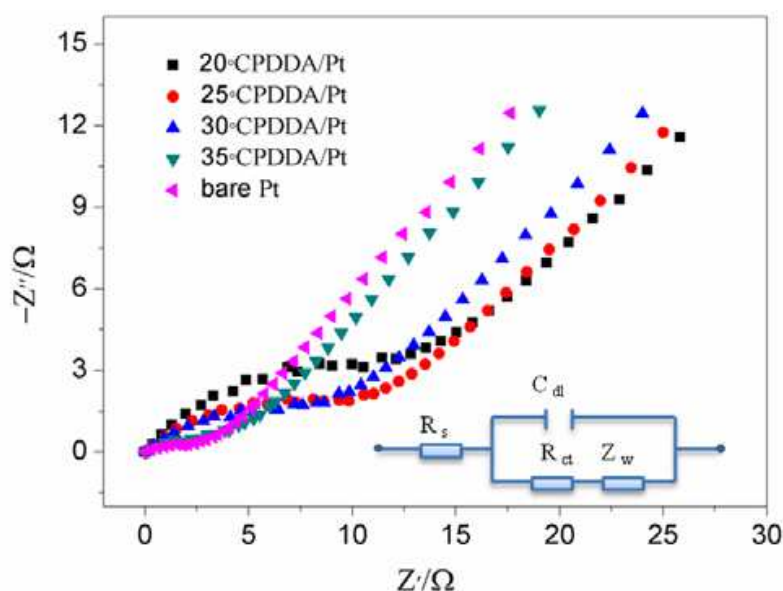


Fig. 2. The EIS diagram for the bare electrode and the electrodes loaded with a PDDA layer at 20, 25, 30, and 35 °C. The inset shows the equivalent circuit used for PDDA modified electrodes, where R_{ct} is the charge transfer resistance, R_s is the solution resistance, Z_w is the Warburg impedance due to the mass transfer from the redox probe to the electrode, and C_{dl} is the double layer capacitance.

Thus, the improvement of electron transport, demands that PDDA is loaded as sparingly as possible. This is because a high loading of PDDA further hinders assembly of PB, which means that a correct loading balance must be achieved.

The affect of PDDA adsorption temperature on PB morphology, and performance, were evaluated to determine the optimum production temperature, and provide a higher electrode performance via the synthesis of a regular PB structure. We investigated whether a regular PB morphology could be achieved by adjusting the PDDA adsorption temperature. Fig. 3 (a) to (d) shows the great differences in surface morphology of PB on modified electrodes, when the PDDA layer was adsorbed at different temperatures. When the PDDA was deposited at 20 °C, the film surface was covered with irregular particles, but the particles grew bigger as the temperature increased to 25 °C. As the temperature increased, the whole surface changed and, instead of irregular particles, an abundance of nanocubes was observed on the electrode surface, with each nanocube measuring ~100 nm. These

regular crystals formed the film and although some nanocubes remained on the surface, the amount decreased. We also measured the PB concentrations on the electrodes. Fig. 3 (e) shows that the PB concentration was 6.059, 6.771, 7.03, and 4.827 nmol cm⁻² at temperatures of 20, 25, 30, and 35 °C, respectively. At the low temperature, the amount of PDDA covering the Pt surface was so large that it caused the aggregation of PB particles. Thus, an excess of crystal nuclei might lead to imperfect growth of PB crystals.

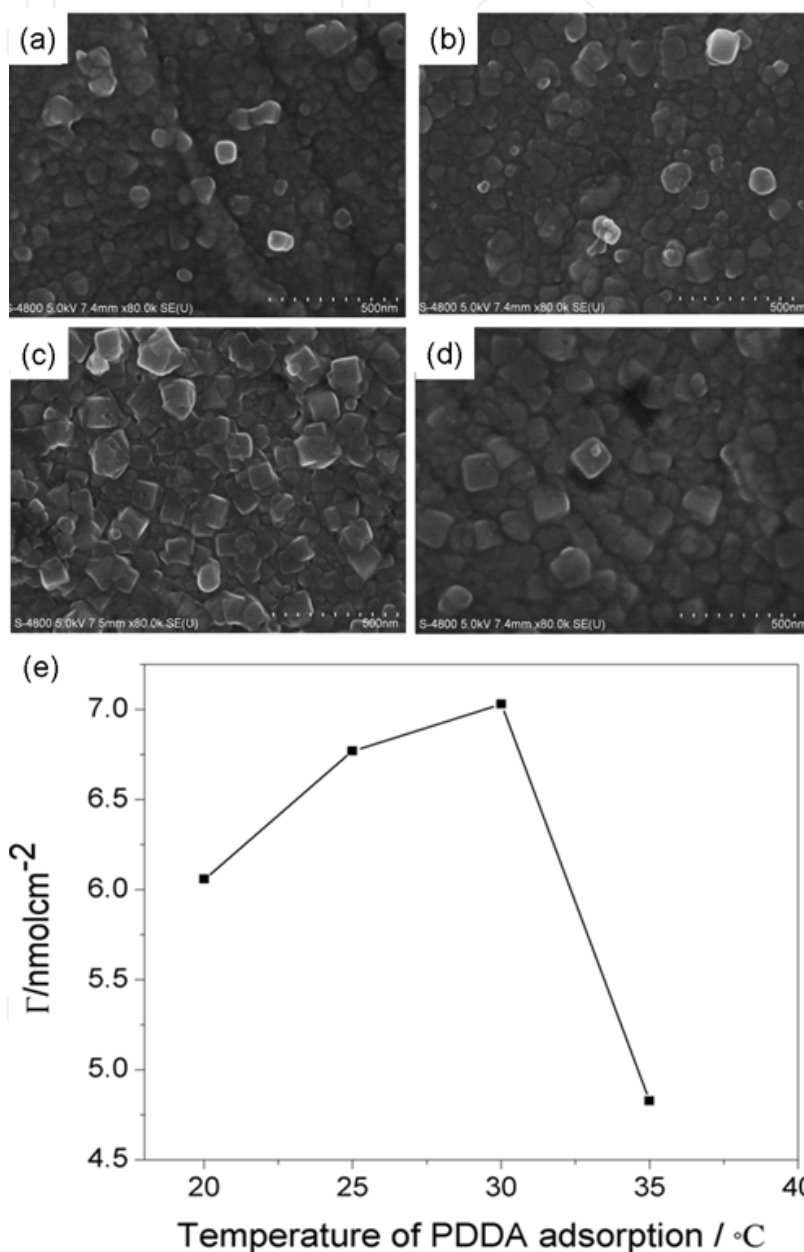


Fig. 3. The FESEM images of PB modified electrodes, where PDDA were adsorbed at different temperatures: (a) 20 °C; (b) 25 °C; (c) 30 °C; (d) 35 °C. (e) Shows the PB concentrations on electrodes at different PDDA adsorption temperature.

The film was comprised of small PDDA particles, which provided adsorption sites for PB assembly. The PB concentration was low at high temperature, because of low PDDA coverage. We showed that a PDDA layer adsorbed at low temperature resulted in a strong

impedance to electron transfer, so we selected 30 °C as the optimal temperature for PDDA adsorption. According to the performance detection procedure, the sensitivity of an electrode prepared at 30 °C was 1179.6 mA M⁻¹ cm⁻², which was much higher than electrodes prepared with no control over PDDA adsorption temperature (Liu et al., 2009).

This improved self-assembly approach to PB film formation successfully produced nanocubic PB crystals and enhanced the sensitivity of H₂O₂ detection. This study demonstrated the constraints on electron transfer impedance imposed by the PDDA layer so we next determined the factors affecting the regular growth of PB in the absence of a polyelectrolyte.

4. Aerosol deposition (AD) for synthesis of PB nanocubes

4.1 Synthesis mechanism

Synthesis of a PB film with a regular morphology, in the absence of polyelectrolyte, demands control of the formation rate during regular PB film growth. Current approaches require PB formation in reactive solutions. However, the concentration of molecules in solution is very high, and PB is produced in seconds when solutions of K₄[Fe(CN)₆] and FeCl₃ are mixed. Thus, it is desirable to achieve PB formation with lower concentration solutions

Aerosols are composed of tiny droplets, which are so small that they are readily suspended in the air. There has been a recent growth in interest in the application of aerosols (Boissiere et al., 2010). The advantages of aerosols are as follows: small volumes lead to micro-reactions and the production of small particles; fewer molecules per unit are required in controlled reactions; the suspension of aerosols avoid the influence of gravity on preparation and promotes uniform growth. We aimed to produce regular PB crystals, without polyelectrolyte, by adopting the AD approach instead of conducting the reaction in solution.

If aerosols are to be used to deposit PB directly onto a Pt electrode, it was essential that an interaction occurred between Pt and reactive aerosols. Before we conducted the experiments, we confirmed that aerosols can be deposited on the electrode surface by virtue of Van der Waals force between the carbon and Pt atoms, according to the results of a Density Functional Theory (DFT) simulation (Chu et al., 2009). This simulation helped us to define the deposition order, i.e., the K₄[Fe(CN)₆] aerosol should be initially attracted onto the Pt surface, because of the carbon conformation. The deposition time of the two aerosols was the same.

4.2 Morphology control

As shown in Fig. 4, aerosols of Fe(CN)₆⁴⁻ and Fe³⁺ were deposited on the Pt surface to form the PB film. The deposition time was a controlled parameter that determined the concentration of aerosols. The small size of liquid used meant that aerosols were more readily affected by environmental temperature, which affected the growth of crystals. Thus, deposition time and temperature were the main controlled factors in the whole process (Chu et al., 2010).

Cyclic voltammetry (CV) experiment showed that the PB concentration on the modified electrode directly correlated with deposition time. Fig. 5 shows the maximal and minimal current values of each curve for the redox peaks of Fe²⁺/Fe³⁺, caused by electron transfer from PB to PW and PW to PB. PB concentrations can be calculated using the data by following equation 3 (Grundler, 2007).

$$\Gamma_T = \frac{Q}{nFA} \quad (3)$$

Where Γ_T represents the concentration of PB, Q is a single peak (either a reduction or oxidation peak), n is the average transfer of electrons calculated by $57/\Delta E$ (ΔE is the difference in potential between the redox potentials), F is the Faraday constant, and A is the area of the electrode.

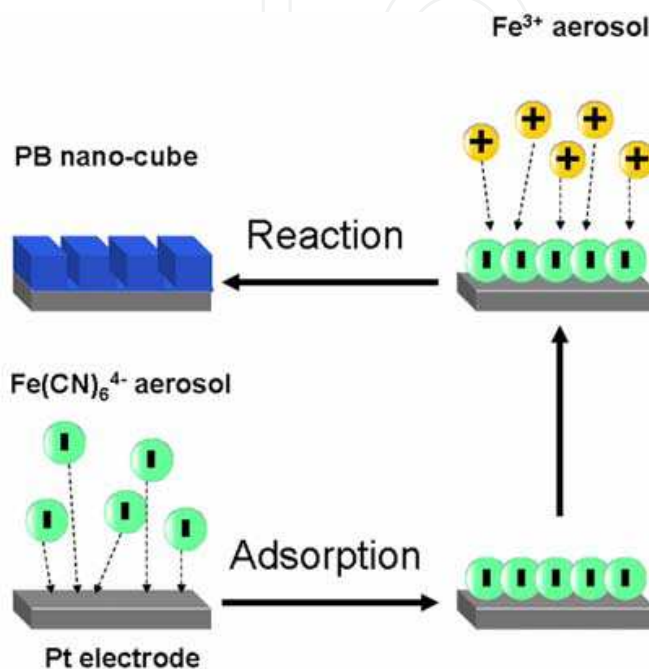


Fig. 4. PB film preparation using the aerosol deposition method.

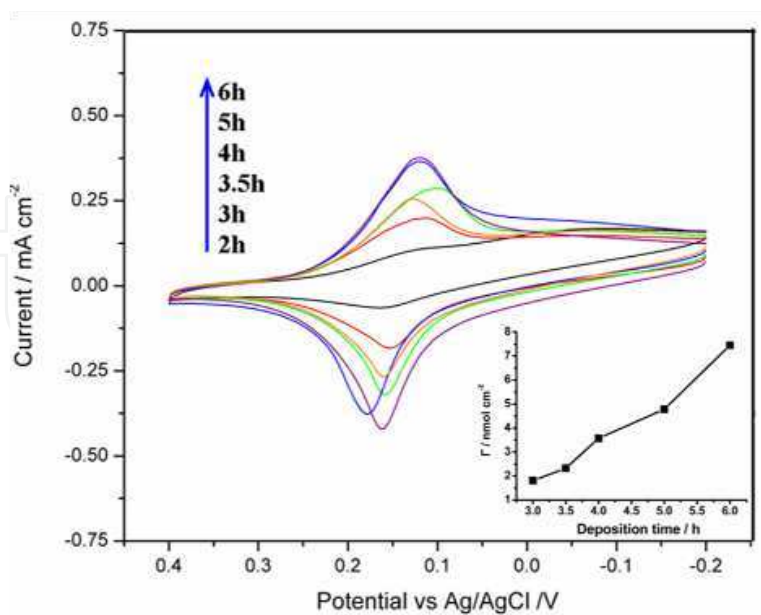


Fig. 5. The CV results for PB-modified electrodes produced for 2, 3, 3.5, 4, 5, and 6 hours. The preparation temperature was kept at 25 °C. The inset shows the diagram of calculated PB concentrations.

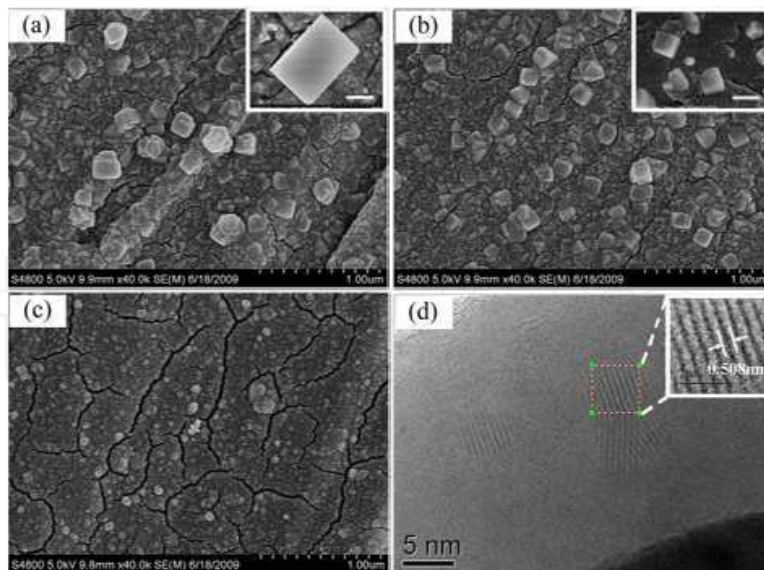


Fig. 6. (a) to (b) Field emission scanning electron microscopy (FESEM) images of PB modified electrodes prepared at 25, 35, and 45 °C. The insets show partial magnified images, where the bar is 250 nm. (d) High resolution transmission electron microscopy (HRTEM) image of an electrode prepared at 35 °C.

The Fig. 5 inset shows the calculated results for PB concentration. Concentration was an approximately linear function of increased deposition time. Thus, the amount of PB on the electrode surface can be finely controlled by the deposition time. The perfect growth of crystals demanded an adequate availability of substrate, so 6 hours was selected as the deposition time constant when investigating the influence of temperature on morphology. We investigated the PB crystal morphology for electrodes prepared at 25, 35, and 45 °C. Fig. 6 shows that regular nanocrystals formed on the electrode surface at 25 and 35 °C. When the film was prepared at 25 °C, the shape of crystal was cuboid-like with a size of ~500 nm, whereas at 35 °C, the crystals were smaller and possessed a more obviously cubic structure. Thus, it was determined that 35 °C was appropriate for the synthesis of larger volumes of crystals with a regular structure. A further increase of the temperature to 45 °C, led to the surface being populated with small particles with an undesirable morphology. Higher temperature also caused serious cracks in the film due to differences of thermal expansion between the PB film and the metal of the Pt electrode. Fig. 7(d) shows an HRTEM image of the growth of crystals produced in one direction, where the d-spacing of the lattice fringes was measured as 0.500 nm, which is consistent with the (200) lattice plane of PB in the PDF card (JCPDS card no.73-0687).

Temperature strongly affects PB morphology, because deposition of aerosols can reduce the amount of molecules available to participate in the reaction. Thus, the driving force of chemical equilibrium is reduced compared to reactions in solution, thereby slowing down the reaction product formation rate. High temperature might accelerate the formation of nuclei for further growth, but the availability of more growth cores could lead to an increase in the amount, but a decrease in the size, of PB crystals. Further problems occur if the temperature is increased further, because the interaction between PB and Pt is governed by the van der Waals force, which is a weak force. Thus, if the temperature is too high molecules will escape from the restraint of interaction due to high thermal motion activity. This can lead to inadequate and imperfect PB crystal growth.

Regular crystals with perfect edges lead to higher sensor performance, because they increase the catalytic activity of biosensors. Thus, a PB electrode with nano-cubic structure is expected to show enhanced sensitivity in the detection of H_2O_2 .

4.3 Performance in H_2O_2 detection

Chronoamperometry is often used in the performance measurement of electrochemical biosensor detection performance. We tested the detection performance of three electrode systems; the Pt electrode we developed as described above, a counter Pt electrode, and an Ag/AgCl electrode. The process was conducted in a phosphate buffer solution (pH = 6.5) to ensure system stability. The potential imposed on the PB modified electrode was - 0.05 V. The stirring was provided to ensure the uniform dispersion of H_2O_2 . After running the baseline, 10 μM H_2O_2 was repeatedly added into the buffer solution at a standard time interval.

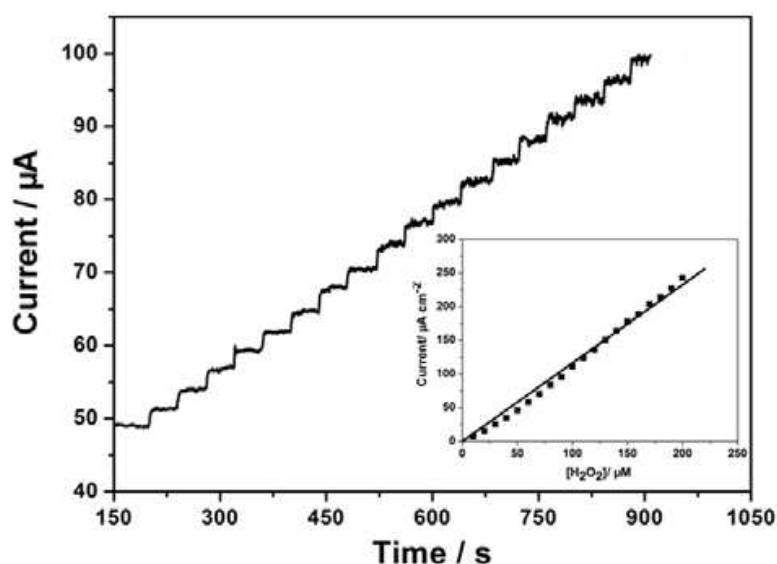


Fig. 7. Current response during H_2O_2 detection. The inset shows a simulation diagram of current versus H_2O_2 concentration.

Fig. 7 shows the change in current after the introduction of H_2O_2 . After 19 treatments of H_2O_2 addition, the step of the current signal remained clear and stable. This shows that the PB construction maintains good stability with an increase of H_2O_2 concentration. The current response data had a linear relationship with the H_2O_2 concentration, which we simulated. The slope of this linear function indicated the H_2O_2 detection sensitivity of the PB modified electrode. The best sensitivity was calculated as $1163 \text{ mA M}^{-1} \text{ cm}^{-2}$. This performance of an electrode prepared using the AD method was higher than traditional preparation methods. The enhancement of sensitivity was attributed to the formation of nanocubic PB crystals. The nanocubes possessed perfect edges, which provided strong electrocatalytic sites for the H_2O_2 reduction. High crystallinity might also provide more PB sites to participate in detection per unit area. Electrons transfer from Fe^{2+} and Fe^{3+} proceeds along a linear pathway $Fe-C \equiv N-Fe$ in the PB unit cell. Thus, the synthesized cube structure matches the PB cell construction of a face-centered cubic lattice, which means that we produced a regular path for electron transport that might decrease the resistance, in terms of geometry.

This production method for performance enhancement was based on the formation of regular structures by decreasing the reaction rate. A common approach for performance improvement depends on the introduction of other compounds with high catalytic ability or favorable conductivity. We confirmed that the AD approach can produce the regular nanocubes of PB, but we further investigated whether the incorporation of other compounds during the production process might further increase the sensitivity. The inclusion of other compounds might affect the growth of PB, and the structure of the film, and further sensitivity improvements might accrue from cooperation between the two materials.

5. Codeposition of a PB-TiO₂ composite film using the AD method

Material selection during biosensor design demands attention to several critical requirements, i.e., non-toxicity, biocompatibility, stability, and cost. Codeposited compounds must also be compatible with PB. Titanium dioxide (TiO₂) is a common material, which satisfies all the required properties and is particularly suited to nanoparticle production, because it is very light. This allows the mixing of powdered TiO₂ with PB aerosols prior to suspension in the air. Synergistic reaction between semiconductors can increase performance, and both of PB and TiO₂ are semiconductors, with energy gaps of 1.58 and 3.2 eV, respectively. The main catalytic function of TiO₂ results from electron excitation of its valence bond to a conduction bond. However, 3.2 eV is a large gap which requires UV light to provide the energy for electron transit. The gap of PB is much lower than that of TiO₂. Combination of these two semiconductors means that they can pad each gap and make excitation easier (Yamamoto, 2009). Thus, doping TiO₂ nanoparticles into the PB film could improve the catalytic ability. This composite design might enhance the H₂O₂ detection sensitivity of the prepared PB electrode.

We next tested the effect of TiO₂ nanoparticle doping into deposition aerosols.

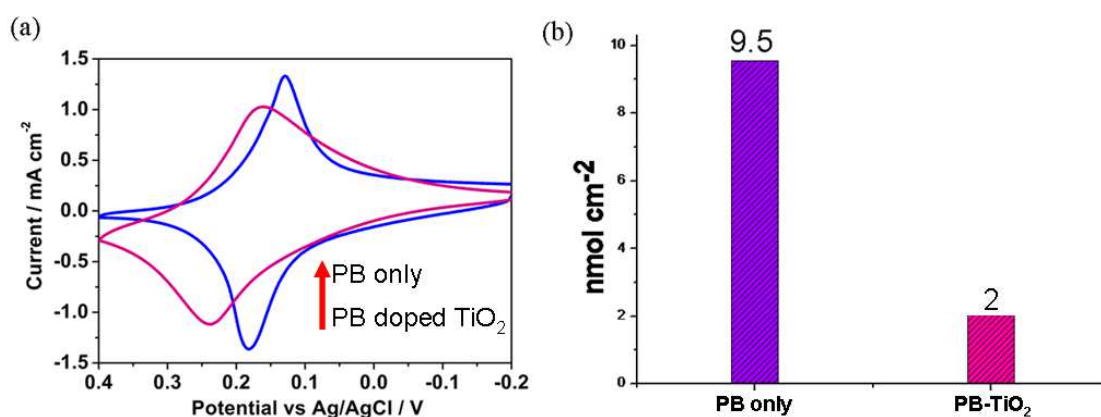


Fig. 8. (a) The comparison of CV diagrams for electrodes with only PB and PB doped with TiO₂. The electrode coating was conducted for 6 hours, at 35 °C. (b) Comparison of calculated PB surface concentrations for both electrodes.

We added 0.1 mmol TiO₂ to the 0.01 mol/L FeCl₃ solution to achieve co-deposition of TiO₂ during the preparation process. The mixed solution was converted to aerosols using an ultrasonic nebulizer. The concentration of TiO₂ was very low because of its poor solubility. Higher amounts would interfere with the ultrasonic method used to produce aerosols. Fig. 8

(a) shows that redox peaks for the electrode with a composite film was lower than that with a PB film. After doping with TiO_2 , the difference between the potentials of oxidation and reduction was larger. The PB concentration was reduced approximately four-fold, according to the calculation results shown in Fig. 8 (b). The deposition of TiO_2 particles in the reactive aerosols, led to them becoming highly packed on the electrode surface, which meant they occupied many growth sites that might have been occupied by PB, after electrode surface adsorption. The interaction between Pt and TiO_2 was very weak. Thus, without the packing of PB particles, TiO_2 particles might easily fall off and detach PB crystals growing around them. This would reduce the concentration of PB on the electrode surface. The widening of the distance between peaks was caused by an increase in electron transfer resistance. Electron transfer through TiO_2 is much harder compared with PB, due to the larger bond gap. The change of concentration might also affect the surface morphology so we investigated the micro-scale surface morphology using FESEM. Fig. 9 (a) shows that the film did not grow fully over the surface. There were numerous flaws on the film surface, making the film discontinuous. The lack of adequate PB prevented correct growth. Compared to the surface morphology shown in Fig. 6(b), the ground film was smooth instead of rough, under the same preparation conditions. However, we found that some nanocubes grew on the ground film, which was very different from the PB-only modified electrode. Nanocubes only grew in the ground film, when the film was only formed of PB crystals, but because of the large size of TiO_2 particles, the PB crystals rapidly aggregated around TiO_2 . PB might struggle to form a regular shape, because of interference from TiO_2 particles, and regular crystals only formed freely on the ground film. The low PB concentration and defects in the film limits any synergistic functionality of PB with TiO_2 , thereby decreasing electrode performance. We prolonged the deposition time in order to form a uniform film and, after increasing the time to eight hours, surface concentration was found to be 5.4 nmol cm^{-2} . Fig. 9 (b) shows that the ground film was uniform and contained no defects. More nanocubes were apparent on the surface and the size increased to $\sim 2 \mu\text{m}$. This was an obvious improvement on electrodes prepared for less than six hours. We compared H_2O_2 detection sensitivity with an electrode prepared under 35°C for six hours.

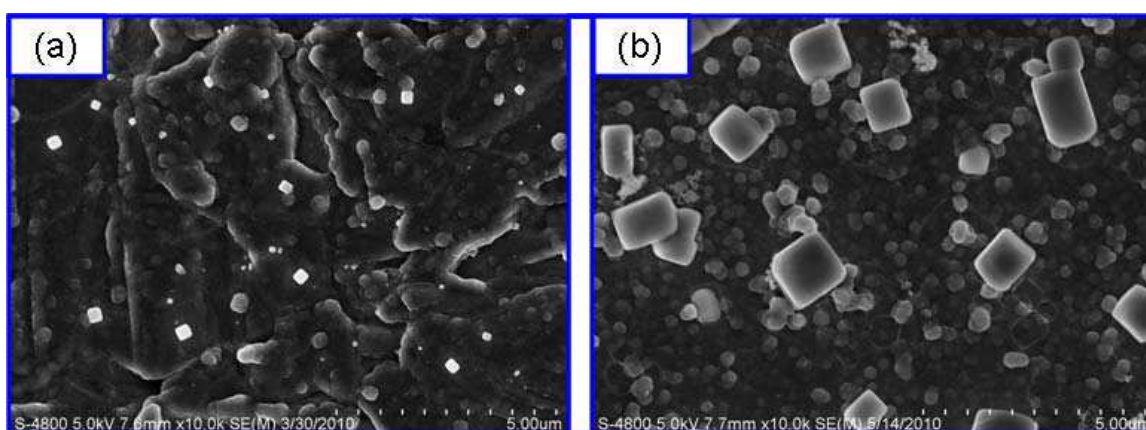


Fig. 9. FESEM images of PB-modified electrodes prepared at 35°C for (a) 6 h, and (b) 8 h.

The introduction of TiO_2 decreased the PB surface concentration and resulted in significant changes in film morphology, particularly the PB crystal shape. This meant that the performance of the prepared PB- TiO_2 composite film was expected to be no improvement on the PB-only film. However, based on the results of H_2O_2 detection (Fig. 10), the

sensitivity was calculated to be $1300 \text{ mA M}^{-1} \text{ cm}^{-2}$, which was a little higher than the PB-only film. This sensitivity is based on a PB concentration that was half that of the PB-only film. The catalytic function of TiO_2 was confirmed. The reductive ability of PB was weakened due to lower PB coverage, but TiO_2 particles contribute to overall catalytic function.

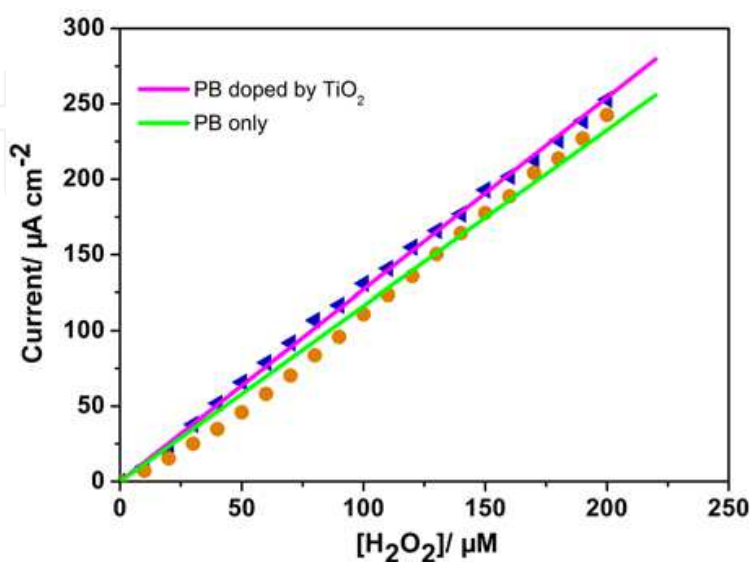


Fig. 10. H_2O_2 detection sensitivity comparison of electrodes with PB-only film and PB- TiO_2 composite film.

This preliminary work confirms that this approach can be applied to the production of regular structures PB and improve the performance of electrodes. Further research includes adjusting the ratio of the doping content and identifying other compounds with better solubility to substitute for TiO_2 .

6. Conclusions and future prospects

Regular nanostructured PB can be synthesized using three methods: self-assembly with temperature controlled polyelectrolyte adsorption, the aerosol deposition approach, and the aerosol co-deposition approach. The regular structured PB film increased detection sensitivity of electrodes. Electron transfer direction in solution is from H_2O_2 to the electrode, and provision of a regular structured pathway for electron transport enhanced the detection efficiency of the modified electrode. This might require the production of oriented structures in the PB film, such as nanotubes or nanowires. However, if this assumption is to be satisfied a template or external force must be applied to set the PB growth direction. An alternative method is to identify compounds to dope the PB film and exploit their synergistic functionality, as we found with TiO_2 . Such methods are not confined to PB fabrication and they may be appropriate in other fields requiring regular crystal synthesis.

7. Acknowledgement

This work was supported by the National Basic Research Program of China (No. 2009CB623406), National Nature Science Foundation of China (No.20990222), The "Six Kinds of Important Talents" Program of Jiangsu province (No.2007007), Innovation Foundation for Doctoral Dissertation of Jiangsu Province (CX09B-133Z).

8. References

- Bartoll, J. (2008). The early use of Prussian blue in paintings, 9th International Conference on NDT of Art, NDT, Jerusalem Israel, pp. 1.
- Boissiere, C., Grosso, D., Chaumonnot, A., Nicole, L. & Sanchez, C. (2010). Aerosol Route to Functional Nanostructured Inorganic and Hybrid Porous Materials, *Advanced Materials*, in press.
- Cao, L., Liu, Y., Zhang, B. & Lu, L. (2010). In situ controllable growth of Prussian Blue nanocubes on reduced graphene oxide: facile synthesis and their application as enhanced nanoelectrocatalyst for H₂O₂ reduction, *ACS Applied Materials & Interfaces*, Vol. 2: 2339–2346.
- Cella, L. N., Chen, W., Myung, N. V. & Mulchandani, A. (2010). Single-walled carbon nanotube-based chemiresistive affinity biosensors for small molecules: ultrasensitive glucose detection, *Journal of the American Chemical Society*, Vol. 132: 5024-5026.
- Chu, Z., Liu, Y., Jin, W., Xu, N., Tieke, B. (2009). Facile fabrication of a Prussian Blue film by direct aerosol deposition on a Pt electrode, *Chemical Communications*, 3566-3567.
- Chu, Z., Zhang, Y., Dong, X., Jin, W., Xu, N., Tieke, B. (2010). Template-free growth of regular nano-structured Prussian blue on a platinum surface and its application in biosensors with high sensitivity, Vol. 20: 7815-7820.
- Grundler, P. (2007). *Chemical Sensors: An Introduction for scientists and Engineers*, Springer-Verlag, Berlin, 2007, ch. 2, pp. 64.
- Guan, N., Sun, D. & Xu, J. (2009). Self-assembly of iron oxide nanoparticles into oriented nanosheets by one-pot template-free synthesis at low pH, *Materials Letters*, Vol. 63: 1272-1274.
- Hornok, V. & Dékány, I. (2007). Synthesis and stabilization of Prussian blue nanoparticles and application for sensors, *Journal of Colloid and Interface Science*, Vol. 309: 176-182.
- Itaya, K., Ataka, T. & Toshima, S. (1982). Spectroelectrochemistry and electrochemical preparation method of Prussian blue modified electrodes, *Journal of the American Chemical Society*, Vol. 104: 4767-4772.
- Karyakin, A. A., Puganova, E. A., Bolshakov, I. A. & Karyakina, E. E. (2007). Electrochemical sensor with record performance characteristics, *Angewandte Chemie International Edition*, Vol. 46: 7678-7680.
- Li, F., Shan, C., Bu, X., Shen, Y., Yang, G. & Niu, L. (2008). Fabrication and electrochemical characterization of electrostatic assembly of polyelectrolyte-functionalized ionic liquid and Prussian blue ultrathin films, *Journal of Electroanalytical Chemistry*, Vol. 616: 1-6.
- Liu, M., Piao, L., Lu, W., Ju, S., Zhao, L., Zhou, C., Li, H. & Wang, W. (2010). Flower-like TiO₂ nanostructures with exposed {001} facets: Facile synthesis and enhanced photocatalysis, *Nanoscale*, Vol. 2: 1115-1117.
- Liu, Y., Chu, Z. & Jin, W. (2009). A sensitivity-controlled hydrogen peroxide sensor based on self-assembled Prussian Blue modified electrode, *Electrochemistry Communications*, Vol. 11: 484-487.
- Liu, Y., Chu, Z., Zhang Y. & Jin, W. (2009). Amperometric glucose biosensor with high sensitivity based on self-assembled Prussian Blue modified electrode, *Electrochimica Acta*, Vol. 54: 7490-7494.

- Millward, R. C., Madden, C. E., Sutherland, I., Mortimer, R. J., Fletcher, S. & Marken, F. (2001). Directed assembly of multilayers—the case of Prussian Blue, *Chemical Communications*, 1994-1995.
- Prevot, V., Forano, C., Khenifi, A., Ballarin, B., Scavetta, E. & Mousty, C. (2011). A templated electrosynthesis of macroporous NiAl layered double hydroxides thin films, *Chemical Communications*, in press.
- Ricci, F. & Palleschi, G. (2005). Sensor and biosensor preparation, optimisation and applications of Prussian Blue modified electrodes, *Biosensors and Bioelectronics*, Vol. 21: 389-407.
- Wang, D., Choi, D., Li, J., Yang, Z., Nie, Z., Kou, R., Hu, D., Wang, C., Saraf, L. V., Zhang, J., Aksay, I. A. & Liu, J. (2009). Self-Assembled TiO₂-Graphene Hybrid Nanostructures for Enhanced Li-Ion Insertion, *ACS Nano*, Vol. 3: 907-914.
- Wang, J. (2008). Electrochemical glucose biosensors, *Chemical Review*, Vol. 108: 814-825.
- Yamamoto, T., Saso, N., Umemura, Y. & Einaga Y. (2009). Photoreduction of Prussian Blue Intercalated into titania nanosheet ultrathin films,
- Zakharchuk, N. F., Meyer, B., Hennig, H., Scholz, F., Jaworksi, A. & Stojek Z. (1995). Comparative study of Prussian-Blue-Modified graphite paste electrodes and solid graphite electrodes with mechanically immobilized Prussian Blue., *Journal of Electroanalytical Chemistry*, Vol. 398: 23-35.

IntechOpen



New Perspectives in Biosensors Technology and Applications

Edited by Prof. Pier Andrea Serra

ISBN 978-953-307-448-1

Hard cover, 448 pages

Publisher InTech

Published online 27, July, 2011

Published in print edition July, 2011

A biosensor is a detecting device that combines a transducer with a biologically sensitive and selective component. Biosensors can measure compounds present in the environment, chemical processes, food and human body at low cost if compared with traditional analytical techniques. This book covers a wide range of aspects and issues related to biosensor technology, bringing together researchers from 12 different countries. The book consists of 20 chapters written by 69 authors and divided in three sections: Biosensors Technology and Materials, Biosensors for Health and Biosensors for Environment and Biosecurity.

How to reference

In order to correctly reference this scholarly work, feel free to copy and paste the following:

Wanqin Jin, Zhenyu Chu and Yannan Zhang (2011). Design and Preparation of Nanostructured Prussian Blue Modified Electrode for Glucose Detection, *New Perspectives in Biosensors Technology and Applications*, Prof. Pier Andrea Serra (Ed.), ISBN: 978-953-307-448-1, InTech, Available from:
<http://www.intechopen.com/books/new-perspectives-in-biosensors-technology-and-applications/design-and-preparation-of-nanostructured-prussian-blue-modified-electrode-for-glucose-detection>

INTECH

open science | open minds

InTech Europe

University Campus STeP Ri
Slavka Krautzeka 83/A
51000 Rijeka, Croatia
Phone: +385 (51) 770 447
Fax: +385 (51) 686 166
www.intechopen.com

InTech China

Unit 405, Office Block, Hotel Equatorial Shanghai
No.65, Yan An Road (West), Shanghai, 200040, China
中国上海市延安西路65号上海国际贵都大饭店办公楼405单元
Phone: +86-21-62489820
Fax: +86-21-62489821

© 2011 The Author(s). Licensee IntechOpen. This chapter is distributed under the terms of the [Creative Commons Attribution-NonCommercial-ShareAlike-3.0 License](#), which permits use, distribution and reproduction for non-commercial purposes, provided the original is properly cited and derivative works building on this content are distributed under the same license.

IntechOpen

IntechOpen